ELSEVIER

Optics Communications 6707 (2000) xxx

OPTICS COMMUNICATIONS

www.elsevier.com/locate/optcom

Numerical analysis and experimental results of output performance for Nd-doped double-clad fiber lasers

Nam Seong Kim [a,b,*], Toshihiro Hamada [a], Mahendra Prabhu [a], Cheng Li [a], Jie Song [a], Ken-ichi Ueda [a], Anping Liu [a], Hong Jin Kong [c]

[a] Institute for Laser Science, University of Electro-Communications, 1-5-1 Chofugaoka, Chofu, Tokyo 182-8585, Japan
[b] Information and Telecommunications Technology Center, The University of Kansas, Lawrence, KA 660047, USA
[c] Department of Physics, Korea Advanced Institute of Science and Technology, Yusong-gu, Taejon 305-701, South Korea

Received 3 March 2000; accepted 17 April 2000

Abstract

Numerical analysis is investigated for the high-power double-clad fiber lasers and experimental results using different microscope objectives for focusing into a Nd-doped rectangular double-clad fiber also performed. The numerical analysis includes dependence of output power on output mirror reflectivity, absorbed pump power, loss, and fiber length and pump power distribution for the cases of one-end and two-end pumps with 20 dB/km loss. Calculated conversion efficiencies are 76.36%, 69.73%, and 63.84% for lossless, two-end pump, and one-end pump fiber lasers, respectively. Slope efficiencies from absorbed pump power/output powers measured using microscope objectives are 16.8%/182 mW, 53.8%/351 mW, 24.9%/1240 mW, and 13.9%/649 mW for magnifications of 5 ×, 10 ×, 20 ×, and 40 ×, respectively.

PACS: 42.55.Wd; 42.55.Xi; 42.60.By
Keywords: Fiber laser; Diode-pumped lasers; Design of specific laser systems; High-power fiber laser; Double-clad fiber laser

1. Introduction

High-power fiber lasers [1–7] have been actively studied in many groups to get compact and comprehensive sources instead of cw Nd-doped crystal lasers for many applications. The high-power fiber lasers have many advantages including very high conversion efficiency, immunity from thermal lensing effect due to large ration of surface area to volume, no need of beam steering, simplicity of optical cavity construction, excellent beam quality, small volume and weight, low cost, and inherently fiber-coupled output. In recent studies, cw 35 W [5] or even 110 W [6] output power at 1120 nm wavelength and no fiber damage at the 110 W power level were reported using Yb-doped rectangular double-clad fiber laser which are very difficult to realize in conventional single-mode fiber lasers. It is theoretically reported there are no important role of nonlinear optical and thermal effects up to as high as 50 W cw powers. The double-clad fiber lasers use clad-pumping tech-

* Corresponding author. Tel.: +1-785-864-7743; fax: +1-785-864-0387; e-mail: knskim@hotmail.com

0030-4018/00/$ - see front matter
PII: S0030-4018(00)00726-4

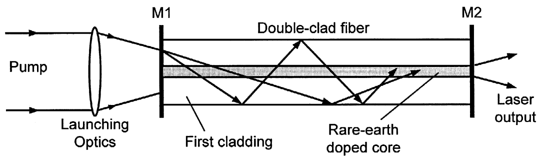

Fig. 1. Schematic diagram of the LD-pumped double-clad fiber laser.

nique, where Nd or Yb-doped core is surrounded by first-cladding and pump light is launched into the first-cladding, propagated inside it, and absorbed by the Nd or Yb in the core when the pump light crosses the core. The conceptual diagram for the double-clad fiber lasers is shown in Fig. 1.

The double-clad fiber lasers have several inherent features including: (a) non-uniformly distributed population inversion due to end-pumping; (b) very high-gain even in a single-pass by a large ratio of gain length to cross-sectional area; and (c) significant distributed losses of the signal light by a long length. Therefore, analytical or numerical analysis on the output performance is essential in order to consider the distributed loss and non-uniform pumping along the fiber length.

In this paper, 'Rigrod analysis' is combined with the model developed by Digonnet [8] to analyze the output performance of the double-clad fiber laser [9]. Firstly, the basic equations on forward and backward powers for the numerical analysis and the related parameters are discussed. Secondly, simulation results on the dependence of the output power are discussed for the output mirror reflectivity, absorbed pump power, fiber loss, and fiber length. Finally, experimental results of the dependence of the output power and the slope efficiency on magnification of focusing microscope objective are included.

2. Equations for forward and backward powers

Previously, various simplifying approximations were performed, but not suitable for double-clad fiber lasers since those ignored the spontaneous emission and even the pump nonuniform effect which dominates the performance of high-power fiber lasers. Since the effective absorption coefficient of the double-clad fibers, the fiber length for an efficient laser operation must be several tens to hundreds meters to achieve 10 dB absorption. To overcome the previous limitation and obtain an exact result, we numerically calculated the power distribution within the fiber, total output power, and other parameters. Regarding this topic, there are several papers published by our group [9,10].

The configuration and parameters for the numerical analysis are shown in Fig. 2 and the governing equations for forward and backward powers and gain factors in a fiber laser cavity are described as [8]:

$$\frac{\mathrm{d}P^{+}(z)}{\mathrm{d}z} = +\frac{\sigma_{\mathrm{s}}\tau_{\mathrm{f}}}{h\nu_{\mathrm{p}}}\alpha_{\mathrm{a}}P_{\mathrm{p}}(0)\mathrm{e}^{-(\alpha_{\mathrm{a}}+\alpha_{\mathrm{p}})z}\frac{F_{\mathrm{p}}}{A_{\mathrm{f}}} \cdot \frac{P_0+P^{+}(z)}{1+(P^{+}(z)+P^{-}(z))/P_{\mathrm{s}}} - \alpha P^{+}(z) \tag{1a}$$

$$\frac{\mathrm{d}P^{-}(z)}{\mathrm{d}z} = -\frac{\sigma_{\mathrm{s}}\tau_{\mathrm{f}}}{h\nu_{\mathrm{p}}}\alpha_{\mathrm{a}}P_{p}(0)\mathrm{e}^{-(\alpha_{\mathrm{a}}+\alpha_{\mathrm{p}})z}\frac{F_{\mathrm{p}}}{A_{\mathrm{f}}} \cdot \frac{P_0+P^{-}(z)}{1+(P^{+}(z)+P^{-}(z))/P_{\mathrm{s}}} + \alpha P^{-}(z) \tag{1b}$$

$$\gamma(z) = \frac{\sigma_{\mathrm{s}}\tau_{\mathrm{f}}}{h\nu_{\mathrm{p}}}\alpha_{\mathrm{a}}P_{p}(0)\mathrm{e}^{-(\alpha_{\mathrm{a}}+\alpha_{\mathrm{p}})z}\frac{F_{\mathrm{p}}}{A_{\mathrm{f}}} \cdot \frac{1}{1+(P^{+}(z)+P^{-}(z))/P_{\mathrm{s}}} \tag{1c}$$

where z measures length along the fiber, $P^{+}(z)$ and $P^{-}(z)$ are forward and backward powers, respec-

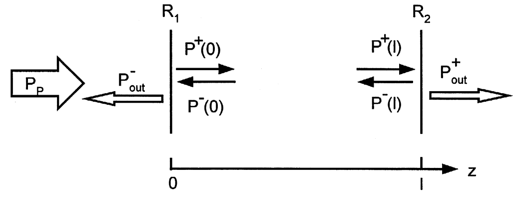

Fig. 2. Configuration for the simulation of the double-clad fiber laser.

tively, $\alpha_a P_p(0)e^{-(\alpha_a+\alpha_p)z}$ is a fractional amount of input pump power $P_p(0)$ absorbed between z and $z+dz$, $\gamma(z)$ is the gain factor along the fiber length, α_a is an effective absorption coefficient of the core at the pump wavelength of λ_p, α_p is a loss coefficient of the fiber at λ_p accounting for all loss mechanisms excluding the resonant absorption described by α_a, σ_s is a stimulated emission cross section, τ_f is a fluorescence lifetime, $h\nu_p$ is the pump photon energy, A_f is the cross-sectional area of the fiber core, F_p is a dimensionless coefficient related to the spatial overlap integral between pump and signal modes [8], α is a loss factor of signal light propagation in the core, $P_s=(h\nu_s/\sigma_s\tau_f)\cdot A_f$ is a saturation output power, and $P_0 = Nh\nu_s\cdot(\pi\Delta\nu_s/2)$ is a constant accounting for spontaneous emissions which is a power associated with N photons in the gain bandwidth $\Delta\nu_s$.

We use parameters for 0.5 wt.% Nd-doped double-clad fiber which is supplied from Mitsubishi Cable. Values of the parameters used in this simulation are $\sigma_s = 2.0\times10^{-24}$ m^2, $\tau_f = 400$ μs, $\lambda_p = 810$ nm, $\lambda_s = 1064$ nm, $\Delta\lambda_s = 30$ nm, $\alpha_a = 180$ dB/km $= 0.0406$ m^{-1}, and $\alpha_s = 10$ dB/km $= 0.0023$ m^{-1}. From those values, $P_0 = 2.36\times10^{-6}\ N$ W and $P_s = 2.32\times10^{8}\ A_f$ W are obtained.

To solve the Eq. (1a) and (1b), some boundary conditions for $P^{\pm}(0)$ and $P^{\pm}(l)$ are needed, but those conditions are not generally available. Here, the boundary conditions for our simulation are found from quasi-conservation condition and compared with boundary values which are found after each iteration. From the Eq. (1a) and (1b), we can easily find a conservation condition for a lossy fiber as follows:

$$\frac{d\left[\left(P_0+P^+(z)\right)\left(P_0+P^-(z)\right)\right]}{dz} = -\alpha P_0\left(P^+(z)-P^-(z)\right). \tag{2}$$

For a lossless fiber, the right-hand term is vanished and the product of 'the forward power plus spontaneous emission' and 'the backward power plus spontaneous emission' becomes a constant over the fiber length. Since P_0 is very small compared to the forward or backward powers, Eq. (2) becomes: $\{dP^+(z)/dz\}/P^+(z) = -\{dP^-(z)/dz\}/P^-(z) =$ gain. It means that the gain is same for the forward and the backward powers. In a lossy fiber, the right-hand term is not vanished and the conservation condition is not satisfied. The loss term makes the product of the forward and the backward powers within the core decreases along z-direction. However, since the right-hand term is very small, the decrease is very slow and it can be assumed that it is negligible. Therefore, we can use the same conservation condition in a lossy fiber as the case in a lossless fiber. Using Eq. (2), $P^+(0) = R_1P^-(0)$, and $P^-(l) = R_2P^+(l)$, a decision condition for the boundary values can be obtained as follows:

$$P^+(l) = \frac{-P_0(1+R_2)+\sqrt{P_0^2(1+R_2)^2+4R_2P^-(0)(P_0+R_2P^-(0)+P_0R_1)}}{2R_2} \tag{3a}$$

$$P^-(0) = \frac{-P_0(1+R_1)+\sqrt{P_0^2(1+R_1)^2+4R_1P^+(l)(P_0+R_2P^+(l)+P_0R_2)}}{2R_1}, \tag{3b}$$

where R_1 and R_2 are reflectivities of left and right mirrors, respectively. Steps for simulation are (I) set initial value on $P^+(0)$; (II) find a corresponding $P^-(0)$ using $P^-(0) = P^+(0)/R_1$; (III) find $P^+(l)$

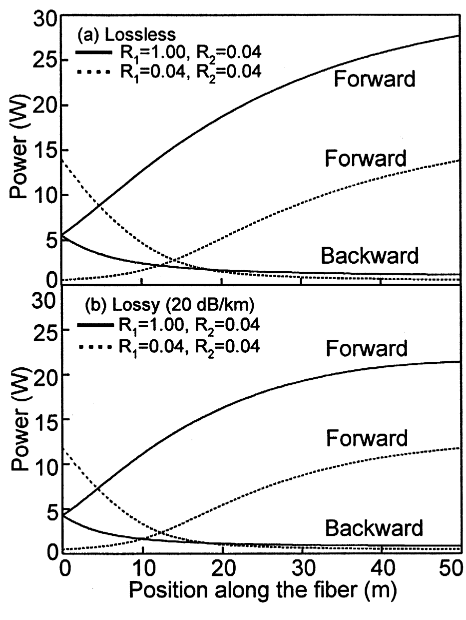

Fig. 3. Evolution of the forward and backward powers along lossless and lossy fiber. $r = 6$ μm and $P_p = 40$ W.

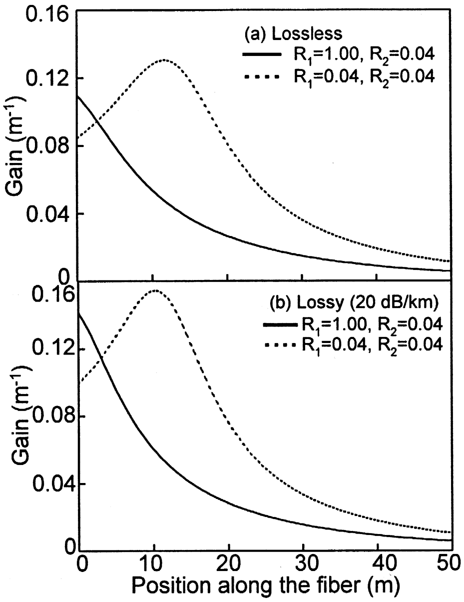

Fig. 4. Evolution of the gain factor along lossless and lossy fiber. $r = 6$ μm and $P_p = 40$ W.

and $P^-(l)$ using a Rounge–Kutta method; (IV) substitute $P^+(l)$ to Eq. (3b); (V) change $P^+(0)$ if $P^-(l)$ obtained from a Rounge–Kutta method is different to the value from Eq. (3b); and (VI) repeat the iterative calculation until it is true.

3. Simulation results and discussion

Evolution of the forward and backward powers along a lossless and a lossy fibers is shown in Fig. 3(a) and 3(b), where a multi-mode double-clad fiber with core radius 6 μm is used and input pump power is 40 W. Mirror reflectivity of 4% is using a cleaved fiber-end surface. In lossy fiber laser, the forward output power for one-mirror cavity is approximately double to that for no-mirror cavity, but 10% less than twice. Therefore, it is expected that two-end pumping generates slightly more output power than one-end pumping. The forward power of 21.4 W for lossy fiber laser is 29% less than that of 27.6 W for lossless fiber laser. The ratio of that decrease is larger than pump power loss ratio which is 20% in 50 m fiber length by fiber loss of 20 dB/km.

Evolution of the gain factor along a lossless and a lossy fibers is shown in Fig. 4(a) and 4(b). For one-mirror cavity, is simply decreasing from left to right end since the total power for the forward and the backward powers near full mirror is low as shown in Fig. 3 and it experiences small-signal gain. However, for no mirror cavity, there is a peak gain position between both ends since a minimum total power is located somewhere along the fiber.

Evolution of total power and gain along the lossy fiber length for right- and left-open cavities is shown in Fig. 5. The forward power is different from the backward power since there is exponential pump power distribution in a lossy fiber. In a right-open cavity, larger absorption of pump power and major gain is obtained near left-end. Therefore, a larger forward power is propagating a longer length of lossy fiber and loses larger amount of power. In a left-open cavity, major gain is still obtained near left-end, but high-power beam is propagating a small length until exiting and amount of loss is relatively small. Therefore, output power in a right-open cavity is larger than that in a left-open cavity.

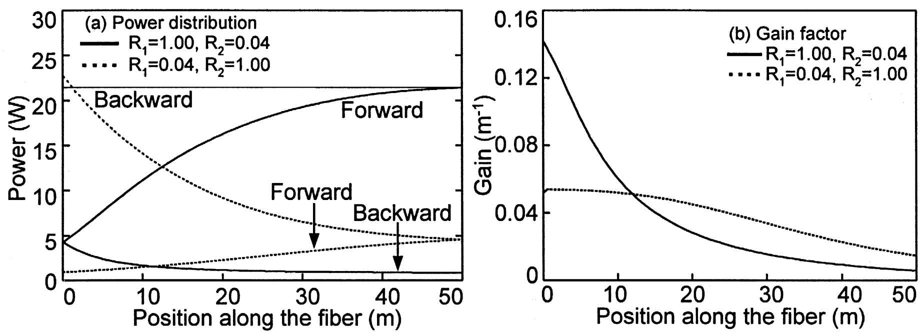

Fig. 5. Evolution of total power and gain factor for lossy double-clad fiber. Loss = 20 dB/km, $r = 6$ μm and $P_p = 40$ W.

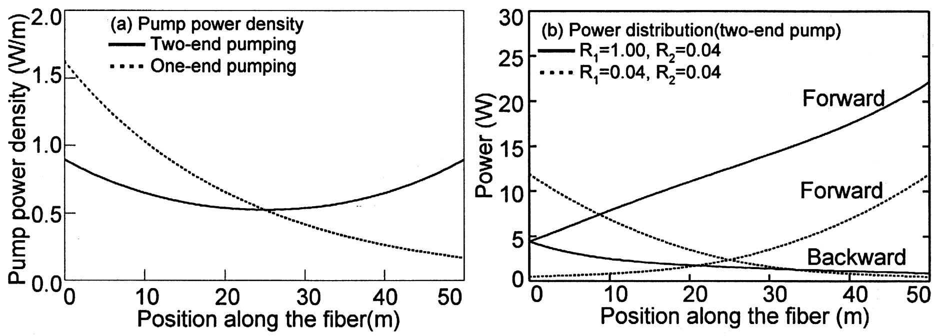

Fig. 6. Pump power density within the fiber and evolution of total power for one-end and two-end pumping. Loss = 20 dB/km, $r = 6$ μm and $P_p = 40$ W.

For one-end and two-end pumping, pump distribution and forward and backward powers are shown in Fig. 6. As we can see in Fig. 6(a), the two-end pumping evens pump distribution along the fiber length. Therefore, distributions of the forward and the backward powers along the fiber length are same for no-mirror cavity in the two-end pumping. For one-end pumping, those are asymmetric due to power dependence of the amount of the fiber loss.

Now let us consider characteristics of the output power for absorbed pump power, fiber loss, reflectivity of output coupler, and fiber length.

Fig. 7 shows the output power versus absorbed pump power for cases of lossless, 10 dB/km loss, and 20 dB/km loss. The core radius of 6 μm, fiber length of 50 m, and pump power of 40 W are used. Slope efficiency is 76.4%, 69.7%, and 63.8% for ideal lossless, 10 dB/km loss, and 20 dB/km loss fibers, respectively. In a lossless fiber laser, photons for almost all of the absorbed pump power are converted to output photons which quantum efficiency is $h\nu_s/h\nu_p = 76.4\%$. In a lossy fiber laser, the signal loss reduces the signal, but the reduced signal experiences higher signal gain. Thus, a loss factor α reduces the output power smaller amount than the ideal factor of $\exp(-\alpha l)$. The slope efficiency expected from the factor of $\exp(-\alpha l)$ is 68.1% and 60.7% for 10 and 20 dB/km, respectively which are smaller than the simulation results of 69.7% and 63.8% for each case.

Fig. 8 shows the output power versus fiber loss at the laser wavelength for one-end pumping with a left-open and a right-open cavities and two-end pumping where the pumping is input through left-end and ‘open’ means the use of cleaved bear-fiber end. The fiber length of 50 m is used. The largest output

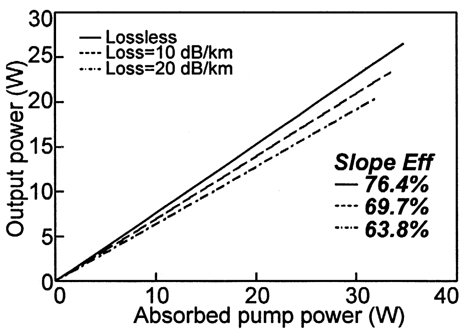

Fig. 7. Output power vs. absorbed pump power for lossless and lossy fibers. $r = 6$ μm, $l = 50$ m, and $P_p = 40$ W.

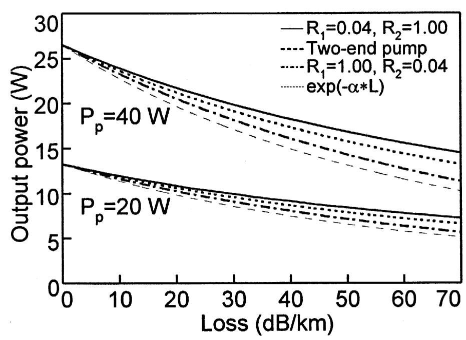

Fig. 8. Output power vs. fiber loss for left/right-open one-end pump and two-end pump using lossy fibers. $r = 6$ μm, $l = 50$ m, and $P_p = 40$ W.

power comes from the one-end pumping with the high reflectivity mirror located far from pumping end. The middle output power comes from the two-end pumping. The lowest output power comes from the one-end pumping with the high reflectivity mirror located near pumping end. The difference between cavities is small for the loss less than 10 dB/km and proportional to the loss. The decrease of the total output power with the loss is less than the ideal factor of $\exp(-\alpha l)$ as it was explained previously.

Fig. 9 shows the output power versus reflectivity of output coupler where reflectivities of 100% and 4% are used for other mirror near pump input side. The fiber length of 50 m are used. The reflectivity of output coupler is varied from 1% to 90% and 40 W and 20 W are used for the pump power. The output coupler is located at the side far from the pump input. In a lossless fiber laser, the output power is almost constant over all range of the reflectivity change since the higher reflectivity increases the power inside the cavity and simultaneously decreases a relative output power. For a lossy fiber laser with left mirror of 100% reflectivity in Fig. 9(a), the higher reflectivity increases a propagation length of the signal due to more round trips and it results in a high loss. Therefore, the output power decreases with the reflectivity of the output coupler and it is believed that the optimum output coupler for high power double-clad fiber laser should have a very low reflectivity. A practical case is an open cavity only with cleaved bare-fiber as output coupler. However, we can use up to 40 or 50% reflectivity if reduction of 10 or 20% in the output power is endurable. For a

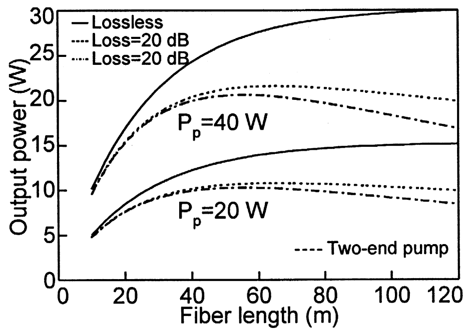

Fig. 10. Output power vs. fiber length for lossless and lossy fibers. Dotted line is for two-end pump and center line for one-end pump. $r = 6$ μm and $P_p = 40$ W.

lossy fiber laser with left mirror of 4% reflectivity in Fig. 9(b), there is also higher loss in case of the higher reflectivity and more loss is experienced due to the low reflectivity at which the mirror of 100% reflectivity is located for Fig. 9(a). When a low reflectivity mirror is used instead of a full mirror at the pump side, there is a steel decrease of the output power with increasing the reflectivity of the output coupler.

Fig. 10 shows the output power versus fiber length for lossless and 20 dB/km loss fibers. The dotted and the center lines are denoted for two-end and one-end pumping using the lossy fiber, respectively. To achieve high absorption efficiency using the double-clad fiber laser, the longer fiber length is preferred since the absorption coefficient of the double-clad fiber is very low. In a lossless fiber laser, the output power increases monotonically with the fiber length and reaches a maximum after pump power is

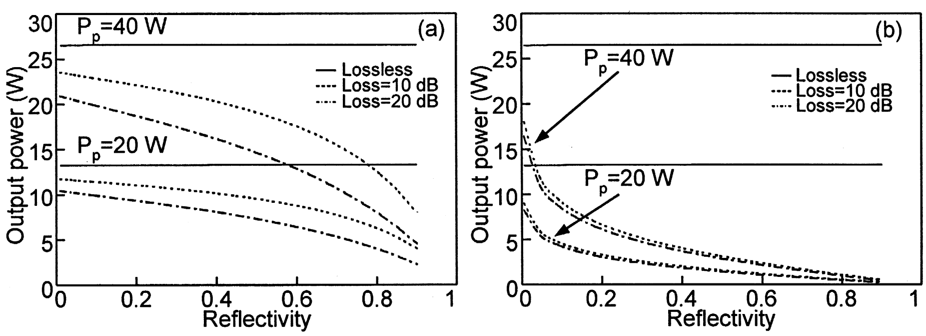

Fig. 9. Output power vs. output mirror's reflectivity. Loss = 0/10/20 dB/km, $r = 6$ μm, $l = 50$ m, and $P_p = 40$ W. (a) $R_1 = 1.00$ and $R_2 =$ vary, and (b) $R_1 = 0.04$ and $R_2 =$ vary.

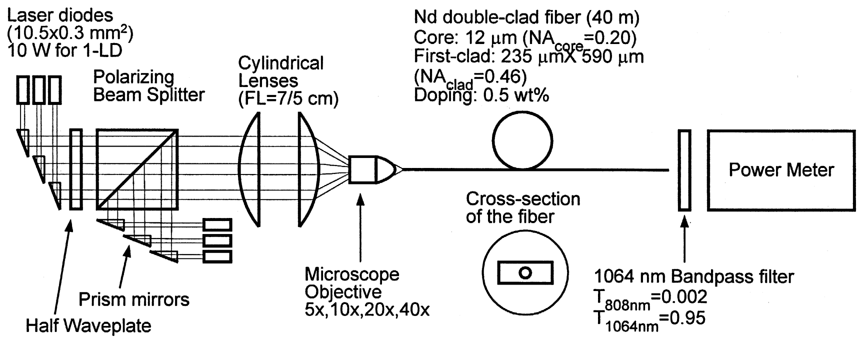

Fig. 11. Experimental setup for Nd-doped rectangular double-clad fiber laser using LD bars with total 40 W focusable power and 5 × (NA = 0.12), 10 × (NA = 0.25), 20 × (NA = 0.40), and 40 × (NA = 0.65) microscope objective.

completely absorbed. In a lossy fiber laser, output power is dependent on the amount of pump absorption and signal loss. Therefore, there is an optimum fiber length to reach a maximum output and the optimum length is mainly dependent on the loss coefficient. In our double-clad fiber laser, 100 m can absorb 98% of pump power with 180 dB/km absorption coefficient. Using a lossless fiber laser, after the fiber length exceeds 100 m, the output power does not change with the fiber length for 40 W and 20 W pump power. However, using the 20 dB/km lossy fiber laser, the output power initially increases with the fiber length and reaches apeak at an optimum length of about 50 m. After then, the output power decreases with the length. Increase of the fiber length makes a larger absorption, but simultaneously adds much larger signal loss. Due to the exponential pump distribution along the fiber length, the signal gain by a longer length than the optimum one is smaller than the signal loss by the longer length. Using a two-end pumping in the lossy fiber laser, the pump distribution is evened and the signal gain is larger than that of one-end pumping. Therefore, the output power can be increased with increasing the fiber length using the two-end pumping.

4. Experiment on dependence of output power and slope efficiency on focusing condition in the Nd-doped rectangular double-clad fiber laser

To understand the dependence of the output power on the focusing condition, we performed an experi-

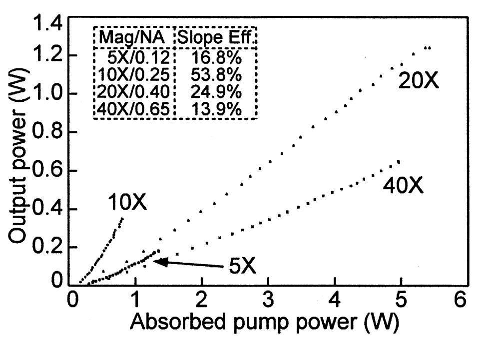

Fig. 12. Output power vs. absorbed power measured for Nd-doped rectangular double-clad fiber laser using focusing optics with various magnification and NA. $r = 6$ μm and $P_p = 40$ W. First clad area and NA are 235 × 590 μm and 0.46, respectively.

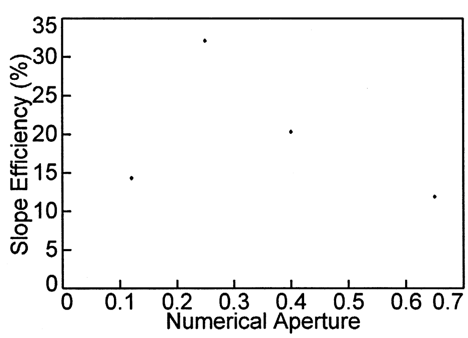

Fig. 13. Slope efficiency vs. NA measured for Nd-doped rectangular double-clad fiber laser. $r = 6$ μm and $P_p = 40$ W. First clad area and NA are 235 × 590 μm and 0.46, respectively.

ment on the Nd-doped double-clad fiber laser using four microscope objectives with 5×, 10×, 20× and 40× magnification which have numerical apertures of 0.12, 0.25, 0.40, and 0.65, respectively. Cleaved bare-fiber ends were used for both sides of laser cavity and fiber length of 40 m was used. The experimental configuration in Fig. 11 is usual one-end pumping scheme that is pumped from left-end. First-clad area and core-diameter are 235 × 590 μm^2 and 12 μm, respectively. Numerical aperture between the first and the second cladding is 0.46. Numerical aperture between the core and the first cladding is 0.20. Nd^{3+} ions in the core are doped with 0.5 wt.%. Absorption coefficient is 180 dB/km. The pump wavelength is 808 nm and the maximum focusable power is 40 W from six laser diode bars. Slope efficiencies measured using microscope objectives are 16.8%, 53.8%, 24.9%, and 13.9% for magnifications of 5×, 10×, 20×, and 40×, respectively. It's maximum output power was 182 mW, 351 mW, 1240 mW, and 649 mW for magnifications of 5×, 10×, 20×, and 40×, respectively. The launched pump power was measured using the double-clad fiber of 1.0 m and the maximum launched power was 1.56 W, 1.22 W, 6.47 W, and 5.54 W for 5×, 10×, 20×, and 40× microscope objective, respectively. The maximum absorbed power was 1.35 W, 0.80 W, 5.43 W, and 4.96 W for 5×, 10×, 20×, and 40× microscope objective, respectively. The maximum launched power and output power were obtained from 20× microscope objective since it's numerical aperture is the best matched with that of the first cladding of the double-clad fiber. However, the maximum slope efficiency was obtained from 10× microscope objective as shown in Figs. 12 and 13. It means that there may be a little difference between the numerical apertures for the best launched power and the best slope efficiency in the double-clad fiber laser. Fig. 14 shows the absorbed versus launched pump powers measured using the four types of microscope objectives. Absorption efficiency is 86.1%, 64.6%, 83.6%, and 89.7% for 5×, 10×, 20×, and 40×, respectively. For this absorption behavior, a further discussion is needed.

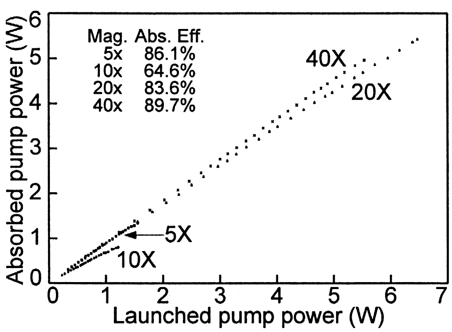

Fig. 14. Absorbed pump power vs. launched pump power measured for Nd-doped rectangular double-clad fiber laser using focusing optics with various magnification and NA. $r = 6$ μm and $P_p = 40$ W. First clad area and NA are 235×590 μm and 0.46, respectively.

5. Conclusions

In conclusion, we have numerically studied about the output characteristics of the Nd-doped rectangular double-clad fiber laser for various design parameters and the experiment on dependence of output power on focusing condition was performed using different microscope objectives. Studied design parameters include output mirror reflectivity, absorbed pump power, fiber loss, fiber length, one-end pump, and two-end pump which were studied for the cases of lossless and lossy fiber laser. The forward and backward power distributions along the fiber length, the gain factor, and the output power are investigated. It is expected that the output power in a right-open cavity is larger than that in a left-open one when the pump power is input from left-end. Two-end pumping evens the distribution of the absorbed pump power and can make more output power than one-end pumping. For the dependence on the fiber loss, there is a small difference in the output powers for several cavities at a small loss, but the differences increase as the loss increases. Therefore, selection of cavity configuration is important in a lossy fiber lasers. For the dependence on the reflectivity of the output coupler, the output power decreases with the reflectivity since larger reflectivity increases a propagation length until the output power exits through the output coupler and makes larger loss. For the mirror in other side in this case, 100% reflectivity can give us a wide selection on the output coupler's reflectivity up to 40–50%, but 4% bare-fiber end can make a steep decrease of the output power with the output coupler's reflectivity. For the dependence on the fiber length, there is an optimum length since the output power does not increase after the pump power is absorbed completely by the fiber.

For the experiment on the dependence on the focusing condition, we used 0.5 wt.% Nd-doped rectangular double-clad fiber which has 12 μm, 235 μm × 590 μm, 800 μm, 40 m for the core diameter, the first-clad size, the second-clad diameter, and the fiber length, respectively. The focusing optics was microscope objective with 5× (NA = 0.12), 10× (NA = 0.25), 20× (NA = 0.40), and 40× (NA = 0.65) magnification. Slope efficiencies/output powers measured using microscope objectives are 16.8%/182 mW, 53.8%/351 mW, 24.9%/1240 mW, and 13.9%/649 mW for magnifications of 5×, 10×, 20×, and 40×, respectively. The maximum slope efficiency was obtained from 10× microscope objective and, therefore, there may be a little difference between the numerical apertures for the best launched power and the best slope efficiency in the double-clad fiber laser.

References

[1] L.A. Zenteno, High-power double-clad fiber lasers, J. Lightwave Technol. 11 (1993) 1435–1446.

[2] A.S. Kurkov, O.I. Medvedkov, V.I. Karpov, S.A. Vasiliev, O.A. Lexin, E.M. Dianov, Photosensitive Yb-doped double-clad fiber for fiber lasers, Tech. Dig. OFC'99, 1999, pp. 205–207.

[3] S.D. Jackson, T.A. King, High-power diode-cladding-pumped Tm-doped silica fiber laser, Opt. Lett. 23 (1998) 1462–1464.

[4] H. Zellmer, U. Willamowski, H. Welling, S. Unger, V. Reichel, H.-R. Muller, J. Kirchhof, P. Albers, High-power cw neodymium-doped fiber laser operating at 9.2 W with high beam quality, Opt. Lett. 20 (1995) 578–580.

[5] M. Muendel, B. Engstrom, D. Kea, B. Laliberte, R. Minns, R. Robinson, B. Rockney, Y. Zhang, R. Collins, P. Gavrilovic, A. Rowley, 35-Watt CW singlemode ytterbium fiber laser at 1.1 μm, Tech. Dig. CLEO'97, Postdeadline paper CPD30, 1997.

[6] V. Dominic, S. MacCormack, R. Waarts, S. Sanders, S. Bicknese, R. Dohle, E. Wolak, P.S. Yeh, E. Zucker, 110 W fibre laser, Electron. Lett. 35 (1999) 1158–1160.

[7] K. Ueda, Outical cavity and future style of high-power fiber lasers, Proc. SPIE 3267 (1998) 14–22.

[8] M.J.F. Digonnet, Theory of superfluorescent fiber lasers, J. Lightwave Technol. 4 (1986) 1631–1639.

[9] A. Liu, K. Kamatani, K. Ueda, Rectangular double-clad fibre laser with two-end-bundled pump, Electron. Lett. 32 (1996) 1673–1674.

[10] A. Liu, K. Ueda, The absorption characteristics of circular, offset, and rectangular double-clad fibers, Opt. Commun. 132 (1996) 511–518.